3D Macrocycles

DOI: 10.1002/ange.201410970

Efficient Synthesis, Structure, and Complexation Studies of Electron-Donating Thiacalix[*n*]dithienothiophene**

Ryota Inoue, Masashi Hasegawa, Tohru Nishinaga, Kenji Yoza, and Yasuhiro Mazaki*

Abstract: *A series of thiacalix[n]dithiothiophenes (n = 4–10) was prepared by a facile method and X-ray analysis was used to determine the molecular structures of square- (4-mer) and pentagonal-shaped macrocycles (5-mer). In the cyclic voltammograms, reversible multielectron redox processes, which are due to electronic delocalization, were observed at low oxidation potentials. The cyclic 4-mer acted as a "Janus-head" cavitand for two C_{60} molecules, whereas the 5- and 6-mer formed stable 1:1 complexes with C_{60}.*

Cyclization reactions to prepare well-defined macrocycles composed of oligoarylene units are usually the most difficult step in many reaction systems.[1] Recently, a variety of synthetic methods have been used to synthesize three-dimensional (3D) hoop-shaped conjugated molecules. Their synthesis usually involves the cyclization of preorganized precursors as the key reaction step.[1d] However, preparation of the particular precursor for cyclization is quite costly, and the need for preorganization hampers comprehensive studies of homologue series with different sizes. Alternatively, simple cyclization of several components affords thermally robust or kinetically reproducible 3D cyclic oligomers, such as cucurbituril, calixarene, and pillerarene.[2,3] Although they can be usually obtained by a one-pot reaction, facile cyclization methods for conjugated macrocycles are still limited with the exception of Rothemund-type synthesis.[4]

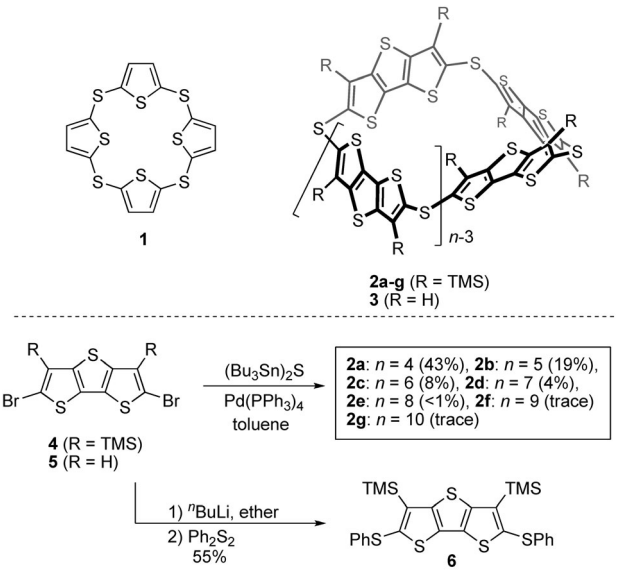

Scheme 1. Synthesis and structures of **1**, **2**, and **6**.

Thiacalix[*n*]thiophenes (**1**; Scheme 1), which are cavitand molecules consisting of thienylene and sulfide linkages, were first reported in the late 1990s by two groups independently.[5] In 1997, König and co-workers reported a one-pot synthesis of thiacalix[*n*]thiophenes from the reaction of a 2,5-thiophene dianion with SCl_2 in a yield of $<1\%$. Soon after that, Nakayama and co-workers developed a more practical multistep synthesis from acyclic precursors (ca. 24% yield). Although these sulfur-bridged oligothiophenes can be used not only as host molecules but also as novel redox-active conjugated molecules, there are few detailed studies of their properties. Bearing in mind the need for an accessible synthesis, we decided to prepare thienylene-containing sulfide-linked 3D macrocycles as a new class of electron-donating cavitand compounds. Here we report the facile and selective synthesis of a series of thiacalix[*n*]dithieno[3,2-*b*:2′,3′-*d*]thiophenes (thiacalix[*n*]DTTs), **2a**–**g** ($n = 4$–10), through a simple Pd-catalyzed coupling reaction of stannyl sulfide.[6] The resulting cyclic oligomers are conjugated through the sulfide linkers, meaning that the electronic properties should depend on the size of the homologue.

An efficient cyclization is shown in Scheme 1. When compound **4**[7] was used as the starting material, the reaction proceeded cleanly to afford various sizes of macrocycles. After purification by gel permeation chromatography (GPC), 4–10 mers **2a**–**g** together with acyclic polymers were obtained.[8] The combined yield of the obtained cyclic homologue series was as high as 75% when toluene was

[*] R. Inoue, Dr. M. Hasegawa, Prof. Y. Mazaki
Department of Chemistry, School of Science
Kitasato University
Sagamihara, Kanagawa 252-0373 (Japan)
E-mail: masasi.h@kitasato-u.ac.jp
Homepage: http://www.kitasato-u.ac.jp/sci/resea/kagaku/HP_kinou/Index.html
Prof. T. Nishinaga
Department of Chemistry
Graduate School of Science and Engineering
Tokyo Metropolitan University
Hachioji, Tokyo 192-0397 (Japan)
Dr. K. Yoza
Bruker AXS
Yokohama, Kanagawa 221-0022 (Japan)

[**] We acknowledge financial support from the Ministry of Education, Culture, Sports, Science, and Technology of Japan through a Grant-in-Aid for Scientific Research (grant number 20438120). We thank Prof. Dr. Takahiro Tsuchiya (Kitasato University) for helpful discussions, and Dr. Yasutoshi Kasahara (Kitasato University) for Raman spectroscopy. All calculations were performed at the Research Center for Computational Science, Okazaki (Japan).

Supporting information for this article is available on the WWW under http://dx.doi.org/10.1002/anie.201410970.

used as the solvent (entry 1; Table 1). When dimethylformamide (DMF) was employed, **2a** precipitated from the reaction mixture. Thus, the formation of the larger macrocycles is suppressed in the catalytic cycle. In fact, the reaction

Table 1: Synthesis of thiacalix[*n*]DTT **2a–c** under various conditions.[a]

Entry	Solvent	Temp.	Yield [%][b]			
			2a	**2b**	**2c**	Others[c]
1	toluene	reflux	43	19	8	< 5
2	DMF	120 °C	56	–	–	–
3	DMF/toluene[d]	120 °C	77	5	2	< 1

[a] 0.5 mmol of **4** and $(Bu_3Sn)_2S$ were used. [b] Yield of isolated product after GPC separation. [c] Sum of other cyclic compounds. [d] v/v = 1:1.

performed in a 1:1 mixture of DMF/toluene showed the highest conversion. In contrast, when the identical cyclization conditions were applied to compound **5**, no cyclization product was obtained, possibly due to low solubility and/or a conformational flexibility of intermediates caused by the absence of bulky TMS groups. Monomeric compound **6** was synthesized for comparison.

Figure 1a shows an X-ray crystal structure of **2a** with chlorobenzene (PhCl).[9] Compound **2a** crystallizes in the tetragonal space group $I4_1/a$ (#88). The four DTT rings are

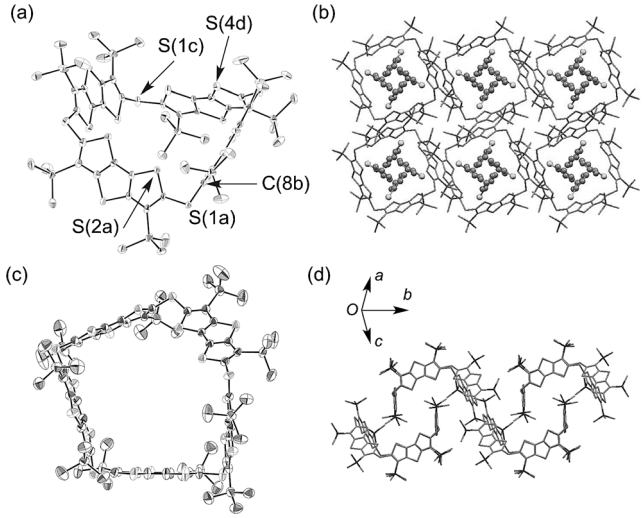

Figure 1. a) ORTEP diagram of **2a**. b) Packing diagram of **2a** and PhCl molecules. c) ORTEP diagram of **2b**. d) Packing diagram of **2b**.

connected together by nonplanar sulfur atoms at the corners. The macrocycle forms a puckered quadrilateral conformation. Adjacent DTT rings are connected in a nearly *anti*-form arrangement through the C–S–C bond to reduce the steric repulsion of the TMS groups so that the macrocycle adopts a nearly 1,3-alternating conformation in comparison to calix[4]arene. Compound **2a** was found to have a large square cavity with a diagonal distance of 12.8 Å (S1a···S1c), and the shortest distance between facing walls was found to be 8.6 Å (S2a···S4d). Although there is no remarkable intermolecular contact between the macrocycles in the packing diagram, **2a** aligns in a channel-like columnar structure along the *c*-axis (Figure 1b). Two PhCl molecules crystallized in the crystal lattice with **2a**.

On the other hand, when there is an odd number of DTT units in the macrocycle, the molecules do not adopt the alternating geometry as a stable conformation due to the steric repulsion among the TMS groups. Compound **2b** has an envelope-shaped pentagonal geometry in which four of the five S atoms at the corners are nearly coplanar (Figure 1c), and the other one is out of the plane.[9] Although the three DTT rings that are confined to the plane of the four S atoms alternate so that their TMS groups are oriented in opposite directions, the other two DTT rings, which are adjacent to each other, align nearly perpendicular to each other. As a result, the macrocycle forms a roughly U-shaped cavity, and one of the DTT rings of the neighboring molecules mutually fills the cavity of the other (Figure 1d). The diagonal S···S lengths of the pentagonal structure were determined to be within the range of 13.2–15.6 Å.

The molecular structures of **2a–c** were calculated by using a DFT method with the B3LYP/6-31G(d) basis set (Figure 2a–c).[10] For **2a**, a molecular geometry, in which four

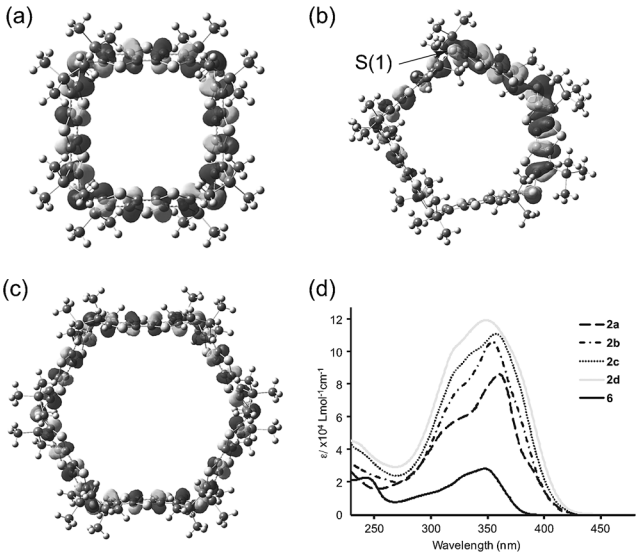

Figure 2. a) HOMOs of **2a**, b) **2b**, and c) **2c**. d) UV/Vis absorption spectra for **2a**, **2b**, **2c**, **2d**, and **6** in CH_2Cl_2.

DTT moieties adopt a 1,3-alternating conformation with D_{2d} symmetry, was found to be a minimum energy structure. On the contrary, from DFT calculations on **2b**, the structure was shown to have a folded arrangement with C_1 symmetry, which is consistent with the X-ray structure. In addition, from DFT calculations, **2c** was determined to have a hexagonal geometry with D_{3d} symmetry (Figure 2c). The lower symmetry in **2b** is attributed to the steric repulsion between the TMS groups at the corners of S(1) (Figure 2b); the parity of the "*n*" results in the structural differences. All of the S atoms of **2a** and **2c** at the corner are almost coplanar, and there is an orbital interaction between the adjacent DTT rings through

the 3p orbitals on the bridged S atoms. For this reason, the HOMO of **2a** and **2c** basically spreads over the cyclic core (Figure 2a and 2c). On the other hand, the coefficients of the HOMO in **2b** are clearly localized within part of the DTT rings due to its envelope-like geometry.

Figure 2d shows UV/Vis absorption spectra for **2a–d** and **6** in CH_2Cl_2. In each spectrum, a similar absorption band with a different molar extinction coefficient was observed. The absorption maxima of **2a** (360 nm), **2b** (355 nm), **2c** (358 nm), and **2d** (349 nm) are red-shifted in comparison to that of **6** (348 nm). These bathochromic shifts are attributed to the conjugation among the DTT units of each macrocycle.

The redox properties of **2a–c** and **6** were investigated by cyclic voltammetry (Figure S18) and differential pulse voltammetry (DPV; Figure 3 and Table 2). In the cyclic voltammograms (CVs) for **2a**, three reversible redox waves were observed at 0.46, 0.54, and 1.00 V. Rotating disk electrode (RDE) analysis on the CVs for **2a** indicated that these redox processes corresponded to $1e^-$, $1e^-$, and $2e^-$ redox processes, respectively. In the CVs of **6**, two $1e^-$ redox processes were observed at 0.52 and 0.86 V. These results indicate that the potentials of the redox processes correspond to the number of sulfide linkages. The first oxidation wave of **2a** is at a lower potential than that of **6**. The lower first potential (E^1_{ox}) implies

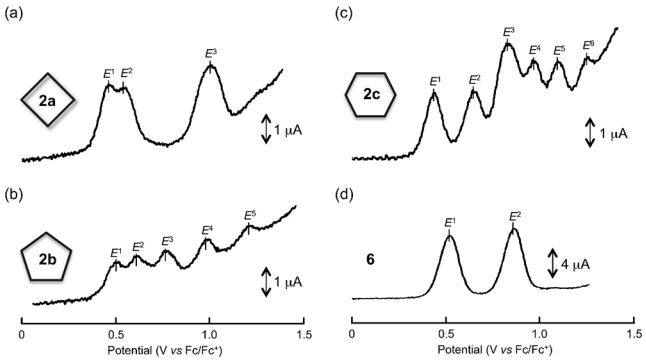

Figure 3. DPV charts for a) **2a**, b) **2b**, c) **2c**, and d) **6**.

Table 2: Redox potentials of **2a–c** and **6** and absorption maxima of their cationic species.[a,b]

Compd.	Redox potentials [V vs. Fc/Fc^+]	Monocation [nm]	Dication [nm]
2a	0.46 ($1e^-$), 0.54 ($1e^-$), 1.00 ($2e^-$)	507, 797 ca. 1500[c]	493, 785
2b	0.50 ($1e^-$), 0.61 ($1e^-$), 0.76 ($1e^-$), 0.98 ($1e^-$), 1.21 ($1e^-$)	508, 806 ca. 1300[c]	503, 798
2c	0.43 ($1e^-$), 0.65 ($1e^-$), 0.83 ($1e^-$), 1.10 ($1e^-$), 1.25 ($1e^-$), 0.96 ($1e^-$)	507, 805 ca. 1600[c]	494, 790
6	0.52 ($1e^-$), 0.86 ($1e^-$)	506, 827	550

[a] All potentials were recorded with DPV in CH_2Cl_2 containing 0.1 M $^nBu_4PF_6$ at 25 °C. Potentials were measured against the Ag/Ag^+ electrode and adjusted to the Fc/Fc^+ potential. [b] Absorption maxima were obtained by using spectroelectrochemistry with a Pt mesh electrode at each potential. [c] Observed as a shoulder.

that $\mathbf{2a}^{\bullet+}$, whose electrons are delocalized due to the conjugation with the corner linkage atoms, forms easily. Subsequently, the second oxidation process leads to the formation of $\mathbf{2a}^{2+}$, and the third oxidation process involves simultaneous two-electron oxidation of $\mathbf{2a}^{2+}$ to $\mathbf{2a}^{4+}$. Electronic spectra of cationic species $\mathbf{2a}^{n+}$ ($1 < n < 4$), generated by spectroelectrochemistry, clearly support the redox processes, described above (Figure S21). Upon oxidation, a broad shoulder absorption band appeared at about 1500 nm due to the delocalized electron among the DTT units, and it disappeared when $\mathbf{2a}^{2+}$ formed.[11] Since the electronic spectra of $\mathbf{6}^{\bullet+}$ exhibited an absorption maximum at 827 nm as the lowest energy band, the observed red-shifts in the spectrum for $\mathbf{2a}^{\bullet+}$ depend on the π-conjugation through the sulfide linkages.

In the CVs of **2b** and **2c**, five and six $1e^-$ reversible redox waves, respectively, were observed. The E^1_{ox} value for **2b** is positively shifted in comparison with those of **2a** and **2c** and is more negative than that of **6**. We think that this is due to the different conjugation of **2b** with a pentagonal U-shaped geometry. In the spectroelectrochemistry, the monocationic species ($\mathbf{2b}^{\bullet+}$ and $\mathbf{2c}^{\bullet+}$) exhibited broad shoulder absorption with tailing to 2000 nm due to the delocalized electron.

Next, we examined the incorporation of C_{60} by **2a–c**. When a solution of **2a** was mixed with C_{60} (> 4 equiv) in $CDCl_3$, the peak corresponding to the TMS protons in ^1H NMR spectra clearly shifted downfield. However, a dark precipitate, which was insoluble in common organic solvents, formed within several minutes. On the contrary, **2b** and **2c** exhibited clear complexation behavior with excess C_{60} in solution. The ^1H NMR signals for both **2b** and **2c** with C_{60} shifted downfield by 0.03 and 0.05 ppm, respectively (Figure 4). Moreover, the ^{13}C NMR signals for C_{60} clearly

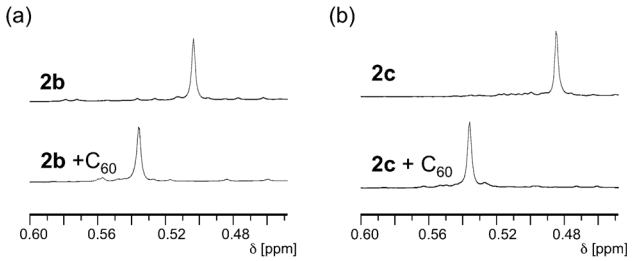

Figure 4. ^1H NMR spectra at room temperature in $CDCl_3$ for a) **2b** and a mixture of **2b** with C_{60}, and b) **2c** and as mixture of **2b** with C_{60}.

shifted upfield (Figure S34).[12] UV/Vis titrations of C_{60} with **2b** or **2c** in PhCl exhibited an increase in the absorption intensity over the range of 400–500 nm upon the addition of each macrocycle solution. On the basis of Job plots, which showed maxima at a molar fraction of 0.5, 1:1 complexes formed in each case. The calculated binding constants (K_a) from the titration experiments, assuming 1:1 complexes, were $(1.6 \pm 0.08) \times 10^3\,M^{-1}$ for **2b** and $(5.3 \pm 0.44) \times 10^4\,M^{-1}$ for **2c**. The larger value of K_a for **2c** indicates facile incorporation of C_{60}. In the optimized D_{3d} geometry of **2c** from the DFT calculations, the distance between opposite DTT rings was ca. 15.5 Å, and thus, the cavity of **2c** is large enough to

incorporate C_{60}. On the other hand, the U-shape geometry of **2b** would somewhat restrain the complexation. Difference spectrum obtained by subtraction of **2b**/**2c** and C_{60} from the absorption of the mixture displays a broad absorption band associated with a weak CT band in the range of 400–650 nm (Figures S39 and S40).[13]

Mixing of **2a** and C_{60} by slow diffusion gave black crystals suitable for X-ray analysis.[9] The crystals contain **2a** and two disordered C_{60} molecules together with *o*-xylene from the solvent in a tetragonal crystal system. The two C_{60} molecules are incorporated in the cavities on each side of **2a** with 1,3-alternating geometry (Figure 5a). Opposite pairs of DTT

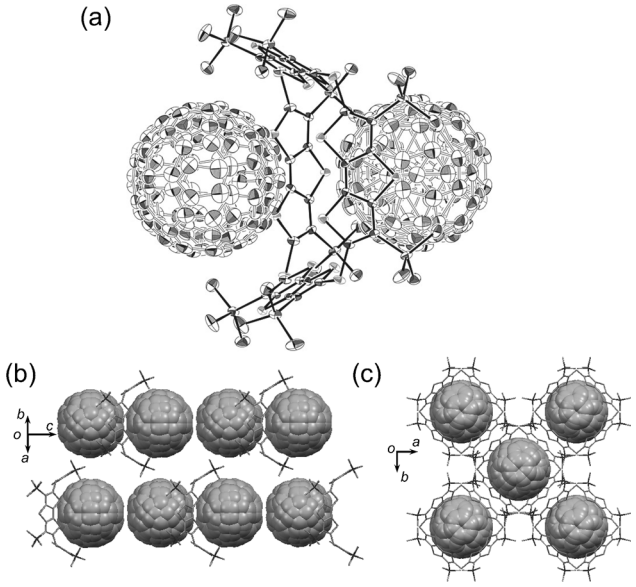

Figure 5. a) X-ray crystal structure of **2a** with two C_{60} molecules. *o*-Xylene molecules are omitted for clarity. b) A columnar array (**2a** and C_{60}) along the *c*-axis. c) C_{60} array in the channel structure.

rings incorporate one C_{60} on each side of the macrocycle. The DTT units capture the C_{60} through π–π interactions as well as sulfur–π contacts. In addition, the TMS groups on both sides of **2a** help hold the C_{60} molecules in the cavities. The Raman and FTIR spectra do not exhibit obvious differences between the crystal and free C_{60}.[14] Since the crystal has an S_4 axis in the center of the macrocycle, the cavities are crystallographically identical, which gives rise to the "Janus-head" in **2a**. Although there are several examples of 1:2 the macrocycle–C_{60} complex, the number of 1:2-complex crystal structures with highly symmetrical orientations is small.[15] In the crystal packing, C_{60} molecules form a 1D-array along the *c*-axis (Figure 5b and c). The high symmetry of the 1:2 complexes allows for the formation of a condensed C_{60} array in the crystal.[16]

In conclusion, we developed an efficient synthesis of a homologue series of thiacalix[*n*]DTT derivatives. From X-ray analysis, **2a** and **2b** were shown to have square and pentagonal shape, respectively. DFT calculations and UV/Vis absorption spectra clearly indicated π-conjugation through the corners. On the bases of CVs and DPVs, the potential of the redox processes depends on the number of sulfide linkages. In the electronic spectra of electrically generated **2a**–**c**$^{+}$, broad absorption bands due to electronic delocalization were observed. Macrocycle **2a** formed a Janus-head complex with two molecules of C_{60}, whereas **2b** and **2c** formed stable 1:1 complexes with C_{60}. The highly symmetrical structure of the Janus-head complex resulted in a condensed 1D array of C_{60} molecules in the crystal.

Received: November 12, 2014
Published online: January 16, 2015

Keywords: cross-coupling · electrochemistry · macrocycles · sulfur heterocycles · supramolecular chemistry

[1] a) M. Iyoda, J. Yamakawa, M. J. Rahman, *Angew. Chem. Int. Ed.* **2011**, *50*, 10522 – 10553; *Angew. Chem.* **2011**, *123*, 10708 – 10740; b) S. Yamago, E. Kayahara, T. Iwamoto, *Chem. Rec.* **2014**, *14*, 84 – 100; c) H. Omachi, Y. Segawa, K. Itami, *Acc. Chem. Res.* **2012**, *45*, 1378 – 1389; d) G. J. Bodwell, *Nat. Chem.* **2014**, *6*, 383 – 385; e) T. Kawase, *Synlett* **2007**, 2609 – 2626.

[2] F. Davis, S. Higson, *Macrocycles: Construction, Chemistry and Nanotechnology Applications*, John Wiley & Sons, Hoboken, **2011**. <

[3] a) J. Lagona, P. Mukhopadhyay, S. Chakrabarti, L. Isaacs, *Angew. Chem. Int. Ed.* **2005**, *44*, 4844 – 4870; *Angew. Chem.* **2005**, *117*, 4922 – 4949; b) T. Ogoshi, T. Yamagishi, *Eur. J. Org. Chem.* **2013**, 2961 – 2975; c) H. Kumagai, M. Hasegawa, S. Miyanari, Y. Sugawa, Y. Sato, T. Hori, S. Ueda, H. Kamiyama, S. Miyano, *Tetrahedron Lett.* **1997**, *38*, 3971 – 3972.

[4] a) E. Vogel, P. Röhrig, M. Sicken, B. Knipp, A. Herrmann, M. Pohl, H. Schmickler, J. Lex, *Angew. Chem. Int. Ed. Engl.* **1989**, *28*, 1651 – 1655; *Angew. Chem.* **1989**, *101*, 1683 – 1687; b) T. Y. Gopalakrishna, J. S. Reddy, V. G. Anand, *Angew. Chem. Int. Ed.* **2014**, *53*, 10984 – 10987; *Angew. Chem.* **2014**, *126*, 11164 – 11167; c) J.-Y. Shin, H. Furuta, K. Yoza, S. Igarashi, A. Osuka, *J. Am. Chem. Soc.* **2001**, *123*, 7190 – 7191.

[5] a) B. König, M. Rödel, I. Dix, P. G. Jones, *J. Chem. Res. Synop.* **1997**, 69; b) J. Nakayama, N. Katano, Y. Sugihara, A. Ishii, *Chem. Lett.* **1997**, 897 – 898; c) N. Katano, Y. Sugihara, A. Ishii, J. Nakayama, *Bull. Chem. Soc. Jpn.* **1998**, *71*, 2695 – 2700.

[6] M. Kosugi, T. Ogata, M. Terada, H. Sano, T. Migita, *Bull. Chem. Soc. Jpn.* **1985**, *58*, 3657 – 3658.

[7] J. Frey, A. D. Bond, A. B. Holmes, *Chem. Commun.* **2002**, 2424 – 2425.

[8] For each compound, simple signals corresponding to their highly symmetrical structures were found. The shape of the signals did not change even at −80 °C except for their chemical shifts.

[9] CCDC 1030028 (**2a**), 1030029 (**2b**), and 1030030 (**2a**-C_{60}), contain the supplementary crystallographic data for this paper. These data can be obtained free of charge from The Cambridge Crystallographic Data Centre via www.ccdc.cam.ac.uk/data_request/cif.

[10] All calculations were performed using Gaussian 09, Revision D.01. M. J. Frisch, et al. Gaussian, Inc.: Willingford, CT, 2009. See Supporting Information for the full citation.

[11] a) F. Zhang, G. Götz, E. Mena-Osteritz, M. Weil, B. Sarkar, W. Kaim, P. Bäuerle, *Chem. Sci.* **2011**, *2*, 781 – 784; b) M. Iyoda, K. Tanaka, H. Shimizu, M. Hasegawa, T. Nishinaga, T. Nishiuchi, Y. Kunugi, T. Ishida, H. Otani, H. Sato, K. Inukai, K. Tahara, Y. Tobe, *J. Am. Chem. Soc.* **2014**, *136*, 2389 – 2396.

[12] We assume that this upfield shift is due to the shielding effects of the DTT walls and/or CT interactions.

[13] Although the present CT absorption band is very weak, dibenzotetrathiafulvalene (DBTTF), whose oxidation potential was found at 0.17 V versus Fc/Fc^+, formed a charge transfer (CT) complex, meaning that CT interactions between the present macrocycles and C_{60} are possible. See D. K. Konarev, R. N. Lyubovskaya, N. V. Drichko, V. N. Semkin, A. Graja, *Chem. Phys. Lett.* **1999**, *314*, 570 – 576.

[14] a) D. V. S. Muthu, M. N. Shashikala, A. K. Sood, R. Seshadri, C. N. R. Rao, *Chem. Phys. Lett.* **1994**, *217*, 146 – 151; b) B. Paci, G. Amoretti, G. Ruani, S. Shinkai, T. Suzuki, F. Ugozzoli, R. Caciuffo, *Phys. Rev. B* **1997**, *55*, 5566 – 5569.

[15] a) S.-X. Fa, L.-X. Wang, D.-X. Wang, L. Zhao, M.-X. Wang, *J. Org. Chem.* **2014**, *79*, 3559 – 3571; b) J. L. Atwood, L. J. Barbour, C. L. Raston, I. B. Sudria, *Angew. Chem. Int. Ed.* **1998**, *37*, 981 – 983; *Angew. Chem.* **1998**, *110*, 1029 – 1031; c) J. Song, N. Aratani, H. Shinokubo, A. Osuka, *Chem. Sci.* **2011**, *2*, 748 – 751.

[16] The single crystal showed no electrical conductivities at room temperature by the two-probe method. Further investigation of the conductivity with other methods are currently underway.

